




RESEARCH ARTICLE

Four-way multimodal fusion of 7 T imaging data using an mCCA+jICA model in first-episode schizophrenia

Kristin K. Lottman¹  | David M. White² | Nina V. Kraguljac² |
Meredith A. Reid³  | Vince D. Calhoun^{4,5}  | Fabio Catao² | Adrienne C. Lahti²

¹Department of Biomedical Engineering, University of Alabama at Birmingham, Birmingham, Alabama

²Department of Psychiatry and Behavioral Neurobiology, University of Alabama at Birmingham, Birmingham, Alabama

³Department of Electrical and Computer Engineering, MRI Research Center, Auburn University, Auburn, Alabama

⁴The Mind Research Network, Albuquerque, New Mexico

⁵Department of Electrical and Computer Engineering, The University of New Mexico, Albuquerque, New Mexico

Correspondence

Adrienne C. Lahti, Department of Psychiatry and Behavioral Neurobiology, University of Alabama at Birmingham, SC 501, 1530 3rd Avenue South, Birmingham, AL 35294-0017, USA.
Email: alahti@uab.edu

Funding information

National Institute of Mental Health, Grant/Award Number: R01 MH102951; Civitan International Research Center, UAB Center for Clinical and Translational Science (CCTS), National Institute of Biomedical Imaging and Bioengineering, Grant/Award Number: R01EB006841; National Institute of General Medical Sciences, Grant/Award Number: P20GM103472; National Science Foundation, Grant/Award Number: IOS 0622318

Abstract

Acquisition of multimodal brain imaging data for the same subject has become more common leading to a growing interest in determining the intermodal relationships between imaging modalities to further elucidate the pathophysiology of schizophrenia. Multimodal data have previously been individually analyzed and subsequently integrated; however, these analysis techniques lack the ability to examine true modality inter-relationships. The utilization of a multiset canonical correlation and joint independent component analysis (mCCA + jICA) model for data fusion allows shared or distinct abnormalities between modalities to be examined. In this study, first-episode schizophrenia patients ($n_{SZ}=19$) and matched controls ($n_{HC}=21$) completed a resting-state functional magnetic resonance imaging (fMRI) scan at 7 T. Grey matter (GM), white matter (WM), cerebrospinal fluid (CSF), and amplitude of low frequency fluctuation (ALFF) maps were used as features in a mCCA + jICA model. Results of the mCCA + jICA model indicated three joint group-discriminating components (GM-CSF, WM-ALFF, GM-ALFF) and two modality-unique group-discriminating components (GM, WM). The joint component findings are highlighted by GM basal ganglia, somatosensory, parietal lobe, and thalamus abnormalities associated with ventricular CSF volume; WM occipital and frontal lobe abnormalities associated with temporal lobe function; and GM frontal, temporal, parietal, and occipital lobe abnormalities associated with caudate function. These results support and extend major findings throughout the literature using independent single modality analyses. The multimodal fusion of 7 T data in this study provides a more comprehensive illustration of the relationships between underlying neuronal abnormalities associated with schizophrenia than examination of imaging data independently.

KEYWORDS

amplitude of low frequency fluctuations, first-episode schizophrenia, joint independent component analysis, multimodal fusion, resting-state fMRI, 7 Tesla

1 | INTRODUCTION

Schizophrenia is often described as a heterogeneous disorder characterized by the presentation of a multitude of different symptoms such as hallucinations, delusions, lack of interest, and anhedonia (Tandon, Nasrallah, & Keshavan, 2009). Owing to the heterogeneity of the disorder, the underlying neural mechanisms and etiology of schizophrenia still remain unclear (Heckers, 2000; Tandon, Keshavan, & Nasrallah, 2008). However, researchers continually attempt to uncover the neural

mechanisms of schizophrenia through studies utilizing structural magnetic resonance imaging (sMRI), functional MRI (fMRI), diffusion tensor imaging (DTI), electroencephalography (EEG), and other imaging modalities (Sui, Yu, He, Pearson, & Calhoun, 2012). Results from different imaging modalities have illustrated increased ventricular volume; volume reductions in the temporal lobe, superior temporal gyrus, and prefrontal cortex (sMRI); neural connectivity abnormalities involving the medial temporal, superior temporal, and prefrontal cortices (DTI); and functional alterations in prefrontal cortex and temporal lobe (fMRI) (see

Keshavan, Tandon, Boutros, & Nasrallah, 2008 for review). Although these results contribute to further understanding the disorder of schizophrenia, the inter-relationships between findings from each modality are relatively unknown.

The acquisition of multiple types of brain imaging data for the same subject has become more common as different imaging modalities provide information about different aspects of the brain, such as functional or structural information (Calhoun & Sui, 2016; Sui et al., 2011). In addition to collecting multiple types of imaging data for an individual, collection of data at higher field strengths (i.e., 7 T) has provided increased spatial resolution and sensitivity to susceptibility effects, as well as decreased T_2^* relaxation times (Moser, Stahlberg, Ladd, & Trattnig, 2012; Poser & Norris, 2009). Even with the collection of multiple imaging modalities at ultra-high resolution, these data are typically analyzed separately for independent results. Although methods where data from one modality are constrained by data from another modality (data integration/conjunction) and *post hoc* pair-wise correlation of independent analysis results have been attempted (Calhoun et al., 2006b; Sui, Huster, Yu, Segall, & Calhoun, 2014), statistics limit the inferences that can be made from these results due to stringent corrections for multiple comparisons, as well as the absence of a common symmetric model to jointly uncover inter-related patterns (Calhoun & Sui, 2016; Sui et al., 2011, 2012). In addition, heterogeneous results have been consistently reported throughout the literature, which may be attributable to only partial detection of disorder abnormalities via single modality analyses (Calhoun et al., 2006b; Calhoun & Sui, 2016; Sui et al., 2011). In order to address these issues, data fusion through the utilization of a multi-set canonical correlation and joint independent component analysis (mCCA + jICA) has been introduced (Sui et al., 2013a).

Joint analysis utilizing the mCCA + jICA model enables the examination of unique and shared variance among multiple modalities and hence illustrates how abnormalities in one modality may influence abnormalities in another (Sui et al., 2013a). Sui and colleagues fused fMRI, DTI, and sMRI to find both joint and modality-unique abnormalities in schizophrenia (Sui et al., 2013b). Among one of the joint components, Sui and colleagues found resting-state fMRI abnormalities in the prefrontal cortex and left superior temporal gyrus were related to grey matter density abnormalities in the motor cortex, temporal gyrus, and medial/superior frontal cortex, along with white matter tract abnormalities of the forceps major, corticospinal tract, and anterior thalamic radiation (Sui et al., 2013b). Wang and colleagues fused resting-state fMRI and sMRI from a large sample of patients with schizophrenia, schizoaffective disorder, and bipolar I disorder with psychosis to find a link between the prefrontal-striatal-thalamic-cerebellar functional networks and default mode network structural abnormalities, and a link between temporal lobe function and structure (Wang et al., 2015). In addition, other joint analyses have found inter-relationships between fMRI auditory oddball task and DTI fractional anisotropy data (Sui et al., 2011); EEG event-related potential and fMRI auditory oddball task data (Calhoun, Adali, & Liu, 2006a); fMRI auditory sensorimotor task, DTI fractional anisotropy, and sMRI grey matter data (Sui et al.,

2013a); as well as many other combinations of schizophrenia multimodal data (see Sui et al., 2014 for review).

In this study, a four-way mCCA + jICA model is utilized in order to examine joint, as well as modality-unique abnormalities in grey matter volume (GM), white matter volume (WM), cerebrospinal fluid volume (CSF), and amplitude of low frequency fluctuations (ALFF) in resting-state fMRI data to discriminate between first-episode patients with schizophrenia and healthy controls. To our knowledge, this is the first study to fuse these four types of imaging data in first-episode schizophrenia patients at 7 T. Based on results from the fusion literature (Calhoun et al., 2006a; Sui et al., 2011, 2013a, 2013b), we expect to see joint, as well as modality-unique, components differentiating first-episode schizophrenia patients from healthy controls. Additionally, we hypothesize that the areas identified in joint and modality-unique components will encompass abnormalities exhibited in single modality analyses for the respective modality; however, we expect that the benefit of this joint analysis approach will be demonstrated with the examination of how abnormalities in one modality are related to and/or influence abnormalities in another via joint components.

2 | MATERIALS AND METHODS

2.1 | Participants

Twenty-two first-episode patients with schizophrenia were recruited from the University of Alabama at Birmingham (UAB) emergency room, inpatient units, and various outpatient clinics. Informed consent to participate in this UAB Institutional Review Board approved study was obtained following evaluation of competency to provide informed consent (Carpenter et al., 2000). Additionally, 22 matched healthy controls, based on age, gender, smoking status, socioeconomic status (SES), and years of education, were enrolled in the study.

Diagnoses were established with review of medical records and evaluation by two board certified psychiatrists (ACL and NVK) and confirmed using the Diagnostic Interview for Genetic Studies (Numberger et al., 1994). All patients were medicated at the time of scanning. Subjects were excluded from the study due to the presence of major medical conditions, neurological disorders, history of head trauma with loss of consciousness, substance abuse within six months of imaging (excluding nicotine), use of medication altering brain function, pregnancy, and MRI contraindications. Exclusion criteria for healthy controls also included a history of Axis I disorders personally or in first-degree relatives.

2.2 | Study design

Participants completed a 6-min (120 volume) resting-state fMRI scan. Of the 22 patients enrolled, one subject was unable to complete the scan due to scanner intolerability; one subject was excluded due to poor scan quality; and a resting-state scan was not obtained for one subject. Therefore, imaging data for 19 patients remained for analysis. Additionally, 21 of the 22 healthy controls enrolled in the study completed a resting-state fMRI scan. Symptom severity was assessed using

the Brief Psychiatric Rating Scale (BPRS) (Overall & Gorham, 1962), the Scale for the Assessment of Negative Symptoms (SANS) (Andreasen, 1984a), and the Scale for the Assessment of Positive Symptoms (SAPS) (Andreasen, 1984b). The Repeatable Battery for the Assessment of Neuropsychological Status (RBANS) (Randolph, Tierney, Mohr, & Chase, 1998) was used to assess cognitive function for healthy controls and patients.

2.3 | Scanning parameters

All scans were performed at the Auburn University MRI Research Center on a whole-body 7 T Siemens MAGNETOM MRI scanner (Siemens Healthineers, Erlangen, Germany), with a 32-channel head coil. High-resolution structural scans were acquired using a three-dimensional T1-weighted magnetization-prepared rapid acquisition gradient-echo sequence (MPRAGE; 256 slices, repetition time/echo time/inversion time [TR/TE/TI] = 2000/2.89/1050 ms, 7° flip angle, 190 mm field of view, 0.7 mm isotropic voxels, base resolution = 256, sagittal acquisition, GRAPPA acceleration factor = 2). Resting-state fMRI scans were acquired using a gradient recalled echo-planar imaging sequence (TR/TE = 3000/28 ms, 70° flip angle, 200 mm field of view, 37 slices, 0.85 mm × 0.85 mm × 1.8 mm voxels, iPAT GRAPPA acceleration factor = 3, base resolution = 234, interleaved acquisition, A > P phase encode direction, 1 ms echo spacing, gap = 1.08 mm). Field maps were acquired using a gradient-recalled echo (GRE) sequence (TR/TE1/TE2 = 400/4.92/7.38 ms, 60° flip angle, 200 mm field of view, 36 slices, 3.1 mm × 3.1 mm × 3.0 mm voxels, base resolution = 64, interleaved acquisition, gap = 0.75 mm).

2.4 | Preprocessing

2.4.1 | Functional magnetic resonance imaging (fMRI)

Data preprocessing of resting-state scans was performed with SPM12 (Wellcome Trust Centre for Neuroimaging, London, UK) and the "CONN" Connectivity Toolbox (Whitfield-Gabrieli & Nieto-Castanon, 2012) using standard preprocessing steps. More specifically, preprocessing steps included realignment and unwarping using phase maps, slice timing correction, coregistration to anatomical space using the T1-weighted MPRAGE structural image and using the first functional image as reference, normalization to Montreal Neurological Institute [MNI] space using the first functional volume as reference, artifact detection, Gaussian smoothing [5 mm full-width half-maximum (FWHM)], and denoising [aCompCor (Behzadi, Restom, Liu, & Liu, 2007), scrubbing, motion regression, linear detrending, and band-pass filtering (0.008–0.09 Hz)]. Volumes were scrubbed if movement exceeded 0.5 mm or noise (z score change > 3) was identified. A smoothed (5 mm FWHM), skull-stripped average whole brain mask of all subjects was utilized as an analysis mask in CONN. Resulting preprocessed functional resting-state data maintained a spatial resolution of 0.855 mm × 0.855 mm × 2.88 mm.

Voxelwise ALFF maps for each subject were extracted from the preprocessed rest data (Song et al., 2011) using the REST toolbox (http://www.restfmri.net/forum/REST_V1.8). More specifically, data

was transformed to the frequency domain with a fast Fourier transform to obtain the power spectrum. ALFF was then calculated (using an average GM mask of all 40 subjects) as the averaged square root of the power spectrum (i.e., amplitude) within a frequency range of 0.01–0.08 Hz.

2.4.2 | Structural magnetic resonance imaging (sMRI)

High-resolution structural scans were segmented into GM, WM, and CSF in SPM12 utilizing an extension of the unified segmentation algorithm (Ashburner & Friston, 2005; Weiskopf et al., 2011). Segmented images were subsequently normalized to MNI space and smoothed with a Gaussian kernel to 5 mm FWHM using the diffeomorphic anatomical registration using exponentiated lie algebra algorithm (DARTEL) (Ashburner, 2007). It is important to note that a more complex intensity nonuniformity field is exhibited among high magnetic field strength (7 T) images compared to the slowly varying intensity nonuniformity profiles exhibited at lower magnetic field strengths (Ganzetti, Wenderoth, & Mantini, 2016b). Therefore, to adequately correct for intensity nonuniformities, optimal input parameters for bias regularization (0.01) and bias field smoothing (30 mm FWHM) were determined utilizing the MRTTool toolbox in SPM12 (Ganzetti, Wenderoth, & Mantini, 2016a) in order to be implemented in the intensity nonuniformity correction methods within the unified segmentation module in SPM12 (Ashburner & Friston, 2005; Ganzetti et al., 2016a). The resultant modulated segmented images representing volume were used in the subsequent analyses as these images correct for deformations that can occur during the spatial normalization process (Fornito, Yucel, Patti, Wood, & Pantelis, 2009). Resulting GM, WM, and CSF maps maintained a spatial resolution of 0.742 mm × 0.742 mm × 0.7 mm.

2.5 | Multiset CCA + joint ICA

We use the mCCA + jICA algorithm as implemented in the fusion ICA toolbox (FIT; <http://mialab.mrn.org/software/fit>). Features entered into the mCCA + jICA model included GM, WM, CSF, and ALFF maps for each individual. Prior to running the mCCA + jICA model, data were normalized in the same manner presented in (Sui et al., 2013b). Three-dimensional feature maps were reshaped to a one-dimensional vector for each subject. The feature vectors for each modality were then stacked to form a subject by number of voxels matrix. Feature matrices were then normalized so that all features had the same mean sum-of-squares. Relative scaling within each modality was preserved following normalization (i.e., 0.3312, 0.2686, 0.1052, 1.4679 for GM, WM, CSF, ALFF, respectively). Following feature normalization, data were reduced via a multi-set canonical correlation analysis (mCCA) (Correa, Li, Adali, & Calhoun, 2008; Sui et al., 2010) and subsequently decomposed into 13 independent components (ICs) via joint independent component analysis (jICA) utilizing the infomax algorithm (Bell & Sejnowski, 1995). The number of components was estimated for each feature (i.e., 11, 13, 23, 4 for GM, WM, CSF, ALFF, respectively) using the minimum description length criteria (Li, Adali, & Calhoun, 2007) and capped at 13 to ensure computational feasibility. Component stability/quality was measured by repeating the infomax algorithm 10 times in

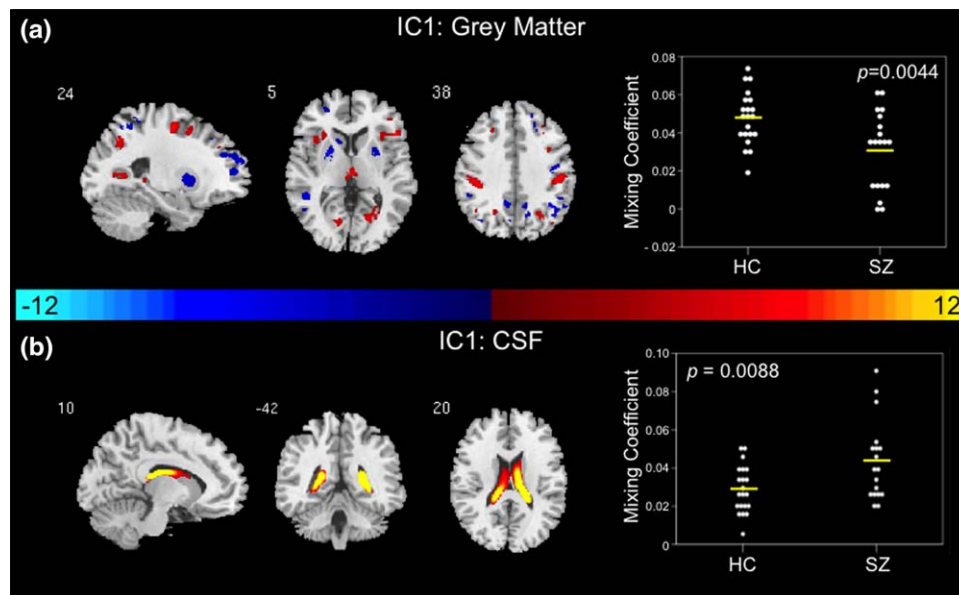


FIGURE 1 Joint group-differentiating IC in Grey Matter and CSF. (a) GM and (b) CSF ICs shown to significantly differentiate between controls and patients via parametric or nonparametric independent samples tests on mixing coefficients. Group differences are found in the two modalities among components with the same indices. Spatial maps are shown with a threshold of $|Z| > 3.5$. A list of the component regions can be found in Supporting Information, Tables I (GM IC1) and III (CSF IC1). (a) Higher mixing coefficients in controls means GM IC1 is expressed more in controls. When GM IC1 z values are positive (red regions) and mixing coefficients are positive, the component is showing increased GM volume in controls. Conversely, when GM IC1 z values are negative (blue regions) and mixing coefficients are positive, the component is showing decreased GM volume in controls. (b) Higher mixing coefficients in patients means CSF IC1 is expressed more in patients. When CSF IC1 z values are positive (red regions) and mixing coefficients are positive the component is showing increased CSF volume in patients. Conversely, when CSF IC1 z values are negative (blue regions) and mixing coefficients are positive, the component is showing decreased CSF volume in patients. IC, independent component; HC, healthy control; SZ, schizophrenia patient; GM, grey matter; CSF, cerebrospinal fluid

ICASSO and the most representative run was used in subsequent steps (Himberg, Hyvarinen, & Esposito, 2004). Components were then z-scored and thresholded at $|Z| > 3.5$ for display. Prior to thresholding for display, components were masked using a GM, WM, or CSF mask (depending on modality; ALFF masked with GM mask) segmented from an average structural image generated from the 40 subjects in the analysis.

2.6 | Mixing coefficients

Subject-specific mixing coefficients or ICA loadings for each modality represent the degree to which a given modality component represents a subject's data as a whole (Lerman-Sinkoff et al., 2017). Based on the normality of the mixing coefficients, either a two-sample *t* test or nonparametric independent samples Mann-Whitney *U* test between mixing coefficients for each respective IC was performed in order to determine group-differentiating components. Normality of mixing coefficients was determined using the Kolmogorov-Smirnov test with Lilliefors correction. Joint group-differentiating ICs are defined as components with the same index exhibiting the ability to differentiate between groups in more than one modality (e.g., IC1 in GM and CSF, IC5 in WM and ALFF, and IC7 in GM and ALFF as shown in Figures 1–3). Joint components have shared variance across modalities (Stephen et al., 2013). A modality-unique group-differentiating IC represents a component in a single modality that demonstrates the ability to differentiate between

groups. Mixing coefficients more than three times the overall interquartile range were identified as outliers and removed. Normality of mixing coefficients was reevaluated prior to calculating two-sample *t* tests or nonparametric independent-samples Mann-Whitney *U* tests to determine group-differentiating components. Three joint components (IC 1 in GM and CSF, IC 5 in WM and ALFF, IC7 in GM and ALFF) and two modality-unique components (IC 3 in WM, IC11 in GM) were identified to significantly differentiate controls and patients. MNI coordinates for voxels with $Z > |3.5|$ and cluster size ≥ 50 in the joint and modality-unique components were extracted using *xjView* (<http://www.alivelearn.net/xjview>) and labeled using the Automated Anatomical Labeling (aal) atlas within *xjView*.

In exploratory *post hoc* analyses, mixing coefficients for the identified significant components were correlated with clinical data including BPRS, SAPS, SANS, and RBANS scores to examine the potential impact of symptoms on the joint and modality-unique components.

3 | RESULTS

3.1 | Demographics

No significant differences in age, gender, parental SES, years of education, and smoking status (packs per day) were exhibited between patients and controls (Table 1). Sixteen patients were treated with risperidone, two with aripiprazole, and one with clozapine.

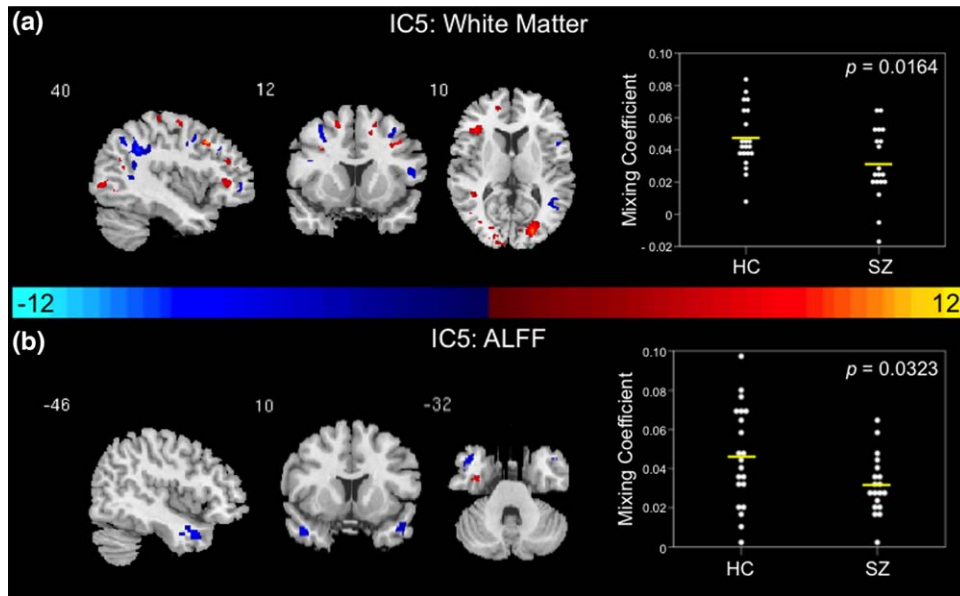


FIGURE 2 Joint group-differentiating IC5 in White Matter and ALFF. (a) WM and (b) ALFF ICs shown to significantly differentiate between controls and patients via parametric or nonparametric independent samples tests on mixing coefficients. Group differences are found in the two modalities among components with the same indices. Spatial maps are shown with a threshold of $|Z| > 3.5$. A list of the component regions can be found in Supporting Information, Tables II (WM IC5) and IV (ALFF IC5). Higher mixing coefficients in controls means WM and ALFF IC5 are expressed more in controls. When WM and ALFF IC5 z values are positive (red regions) and mixing coefficients are positive, the component is showing increased WM volume/ALFF in controls. Conversely, when WM and ALFF IC5 z values are negative (blue regions) and mixing coefficients are positive, the component is showing decreased WM volume/ALFF for controls. The opposite is true when mixing coefficients are negative. IC, independent component; HC, healthy control; SZ, schizophrenia patient; WM, white matter; ALFF, amplitude of low frequency fluctuations

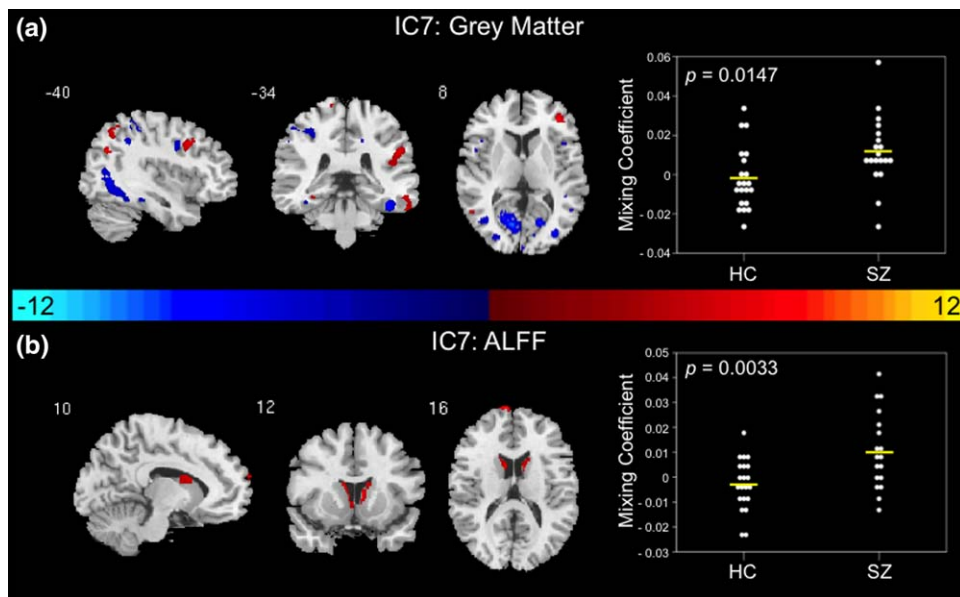


FIGURE 3 Joint group-differentiating IC7 in grey matter and ALFF. (a) GM and (b) ALFF ICs shown to significantly differentiate between controls and patients via parametric or nonparametric independent samples tests on mixing coefficients. Group differences are found in the two modalities among components with the same indices. Spatial maps are shown with a threshold of $|Z| > 3.5$. A list of the component regions can be found in Supporting Information, Tables I (GM IC7) and IV (ALFF IC7). Higher mixing coefficients in patients means GM and ALFF IC7 is expressed more in patients. When z values (red regions) are positive and mixing coefficients are positive, the component is showing increased GM volume/ALFF in patients. Conversely, when GM and ALFF IC7 z values are negative (blue regions) and mixing coefficients are positive, the component is showing decreased GM volume/ALFF in patients. The opposite is true when mixing coefficients are negative. IC, independent component; HC, healthy control; SZ, schizophrenia patient; GM, grey matter; ALFF, amplitude of low frequency fluctuations

TABLE 1 Demographics and clinical assessments^a

	HC (n = 21)	SZ (n = 19) ^b	t/ χ^2	p value
Age (years)	23.48 ± 4.46	22.95 ± 4.39	0.377	0.708
Gender (male/female)	16/5	14/5	0.033	0.855
Parental SES ^c	3.38 ± 3.28	4.61 ± 4.47	5.871	0.555
Education ^d	3.10 ± 0.54	2.83 ± 0.62	2.351	0.309
Smoking (packs per day)	0.00 ± 0.00	0.08 ± 0.16	-2.109	0.050
Duration of Illness (months)	-	18.94 ± 27.40	-	-
BPRS ^e (n = 17)				
Total score	-	30.41 ± 8.41		
Positive symptom subscale	-	4.76 ± 2.73		
Negative symptom subscale	-	5.65 ± 2.32		
SANS ^f (n = 15)				
Total composite score ^g	-	21.50 ± 19.13		
Global summary score	-	6.53 ± 5.29		
SAPS ^h (n = 15)				
Total composite score	-	7.93 ± 12.33		
Global summary score	-	2.73 ± 3.63		
RBANS ⁱ				
Total index	94.78 ± 8.63	75.00 ± 16.16	4.26	<0.001
Immediate memory	99.61 ± 13.10	80.27 ± 15.55	3.88	<0.001
Visuospatial	89.17 ± 14.01	81.60 ± 17.63	1.37	0.1792
Language	105.22 ± 10.85	82.80 ± 11.45	5.77	<0.001
Attention	96.67 ± 14.46	74.53 ± 21.26	3.55	0.0013
Delayed memory	92.06 ± 8.90	82.27 ± 18.46	1.88	0.0753

Note. Abbreviations: HC = healthy control; SZ = schizophrenia; SES = socioeconomic status; Y = yes; N = no; BPRS = Brief Psychiatric Rating Scale; SANS = Scale for the Assessment of Negative Symptoms; SAPS = Scale for the Assessment of Positive Symptoms; RBANS = Repeated Battery for the Assessment of Neuropsychological Status.

^aMean ± SD unless otherwise indicated.

^bSZ values for SES, education, smoking (packs per day), and duration of illness (months) calculated with *n* = 18 due to data missing for one patient.

^cSES ranks reported from Diagnostic Interview for Genetic Studies scale (1–18); high rank (lower numerical value) corresponds to high socioeconomic status.

^dYears of education reported from Diagnostic Interview for Genetic Studies scale.

^eBPRS reported on 1–7 scale; positive (conceptual disorganization, hallucinatory behavior, and unusual thought content); negative (emotional withdrawal, motor retardation, and blunted affect).

^fSANS includes five subscales: affective flattening or blunting, alogia, avolition-apathy, anhedonia-asociality, and attention.

^gSANS average total composite score calculated with data from 14 SZ due to missing data from one SZ.

^hSAPS includes four subscales: hallucinations, delusions, bizarre behavior, and positive formal thought disorder.

ⁱRBANS data missing from 3 HC (*n* = 18) and 4 SZ (*n* = 15).

Information on patient symptom scores can be found in Table 1. In addition, patients exhibited significantly lower immediate memory, language, attention, and total RBANS scores in comparison to controls (Table 1).

3.2 | Joint components

Results of two-sample *t* tests and nonparametric independent-samples Mann–Whitney U tests on IC mixing coefficients indicated three joint

group-differentiating components. These components included IC1 in GM and CSF, IC5 in WM and ALFF, and IC7 in GM and ALFF.

3.2.1 | Grey matter and cerebrospinal fluid

A joint group-differentiating component in GM and CSF was identified based on results of two-sample *t* tests and nonparametric independent-samples tests on the mixing coefficients of IC1. Controls demonstrated higher average GM mixing coefficients in IC1 (*t* = 3.074, *p* = .0044) in comparison to patients (Figure 1a). Conversely, patients

exhibited higher average CSF mixing coefficients in IC1 ($t = -2.765$, $p = .0088$) than controls (Figure 1b). It is important to note that a single patient outlier in the CSF mixing coefficients in IC1 was removed prior to implementing a two-sample t test on the mixing coefficients (reflected in the plot of mixing coefficients in Figure 1b). The mixing profiles of IC1 in GM and CSF were significantly correlated ($r = -0.562$, $p < .001$). Joint group-differentiating IC1 maps for GM and CSF are illustrated in Figure 1a,b. In the GM IC1 spatial map illustrated in Figure 1a, higher mixing coefficients in controls means GM IC1 is expressed more in the data of controls. Additionally, if GM IC1 z values are positive (red regions) and mixing coefficients are positive, this means the component was showing increased GM volume in controls. Conversely, if GM IC1 z values are negative (blue regions) and mixing coefficients are positive, this means the component was showing decreased GM volume in controls. The opposite is true when mixing coefficients are negative. In the CSF IC1 spatial map illustrated in Figure 1b, higher mixing coefficients in patients means CSF IC1 is expressed more in the data of patients. Additionally, if CSF IC1 z values are positive (red regions) and mixing coefficients are positive, this means the component was showing increased CSF volume in patients. Conversely, if CSF IC1 z values are negative (blue regions) and mixing coefficients are positive, this means the component was showing decreased CSF volume in patients. The opposite is true when mixing coefficients are negative. A full list of the regions identified in the joint GM and CSF IC1 are summarized in Supporting Information, Tables I and III, respectively. Multi-slice views of GM and CSF IC1 can be found in Supporting Information, Figure 1. The relationship between the regions from the joint IC1 are shown in the group average difference histogram in Supporting Information, Figure 2.

3.2.2 | White matter and ALFF

A joint group-differentiating component including WM and ALFF in IC5 was determined based on results of two-sample t tests. Controls demonstrated higher average WM ($t = 2.511$, $p = .0164$) and ALFF ($t = 2.236$, $p = .0323$) mixing coefficients in IC5 in comparison to patients (Figure 2a,b). In the WM and ALFF IC5 spatial maps illustrated in Figure 2a,b, higher mixing coefficients in controls means WM and ALFF IC5 is expressed more in the data of controls. Additionally, if WM and ALFF IC5 z values are positive (red regions) and mixing coefficients are positive, this means the component was showing increased WM volume or ALFF in controls. Conversely, if WM and ALFF IC5 z values are negative (blue regions) and mixing coefficients are positive, this means the component was showing decreased WM volume or ALFF in controls. The opposite is true when mixing coefficients are negative. All of the regions identified in the joint WM and ALFF IC5 are listed in Supporting Information, Tables II and IV, respectively. Multislice views of WM and ALFF IC5 can be found in Supporting Information, Figure 3. The relationship between the regions from the joint IC5 are shown in the group average difference histogram in Supporting Information, Figure 4.

3.2.3 | Grey matter and ALFF

A GM and ALFF joint group-differentiating component was determined based on results of two-sample t tests and nonparametric independent-samples tests on the mixing coefficients of IC7. First-episode schizophrenia patients demonstrated higher average GM ($t = -2.556$, $p = .0147$) and ALFF ($t = -3.141$, $p = .0033$) mixing coefficients in IC7 compared to controls (Figure 3a,b). It is important to note that a single patient outlier in the ALFF mixing coefficients in IC7 was removed prior to implementing a two-sample t test on the mixing coefficients (reflected in the plot of mixing coefficients in Figure 3b). In the GM and ALFF IC7 spatial maps (Figure 3a,b), higher mixing coefficients in patients means GM and ALFF IC7 is expressed more in the data of patients. Additionally, if GM and ALFF IC7 z values are positive (red regions) and mixing coefficients are positive, this means the component was showing increased GM volume or ALFF in patients. Conversely, if GM and ALFF IC7 z values are negative (blue regions) and mixing coefficients are positive, this means the component was showing decreased GM volume or ALFF in patients. The opposite is true when mixing coefficients are negative. A full list of the regions identified in the joint GM and ALFF IC7 are shown in Supporting Information, Tables I and IV, respectively. Multislice views of GM and ALFF IC7 can be found in Supporting Information, Figure 5. The relationship between the regions from the joint IC7 are shown in the group average difference histogram in Supporting Information, Figure 6.

3.3 | Modality-unique components

Results of two-sample t tests and nonparametric independent-samples Mann-Whitney U tests on IC mixing coefficients indicated two modality-unique components. These components included IC3 in WM and IC11 in GM.

3.3.1 | White matter

Results of a two-sample t test on component mixing coefficients from IC3 indicated a WM modality-unique group-differentiating IC. First-episode patients with schizophrenia demonstrated significantly higher average mixing coefficients in comparison to controls ($t = -2.121$, $p = .0405$). Therefore, in the spatial map for WM IC3 illustrated in Figure 4a, higher mixing coefficients in patients means WM IC3 is expressed more in the data of patients. Additionally, if WM IC3 z values are positive (red regions) and mixing coefficients are positive, this means the component was showing increased WM volume in patients. Conversely, if WM IC3 z values are negative (blue regions) and mixing coefficients are positive, this means the component was showing decreased WM volume in patients. The opposite is true when mixing coefficients are negative. The regions identified in the modality-unique WM IC3 are listed in Supporting Information, Table II. Multislice views of WM IC3 can be found in Supporting Information, Figure 7A.

3.3.2 | Grey matter

A GM modality-unique group-differentiating IC was identified based on results of a two-sample t test on component mixing coefficients from IC11. Results indicated significantly higher average mixing coefficients

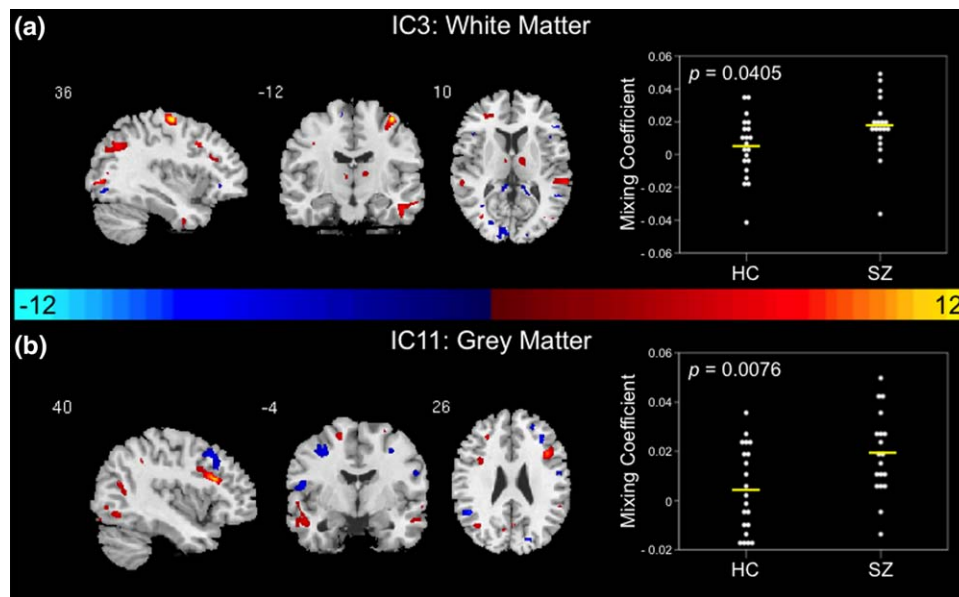


FIGURE 4 Modality-unique components. (a) WM IC 3 and (b) GM IC11 are shown to significantly differentiate between controls and patients via parametric or nonparametric independent samples tests on mixing coefficients. Group differences are found in individual modalities among components with different indices. Spatial maps are shown with a threshold of $|Z| > 3.5$. A list of the component regions can be found in Supporting Information, Tables I (GM IC11) and II (WM IC3). Higher mixing coefficients in patients means WM IC3 and GM IC11 are expressed more in patients. When z values (red regions) are positive and mixing coefficients are positive, the component is showing increased WM/GM volume in patients. Conversely, when WM IC3 and GM IC11 z values are negative (blue regions) and mixing coefficients are positive, the component is showing decreased WM/GM volume in patients. The opposite is true when mixing coefficients are negative. IC, independent component; HC, healthy control; SZ, schizophrenia patient; WM, white matter; GM, grey matter

in patients compared to controls ($t = -2.820$, $p = .0076$). Therefore, in the spatial map for the GM IC11 illustrated in Figure 4b, higher mixing coefficients in patients means GM IC11 is expressed more in the data of patients. Additionally, if GM IC11 z values are positive (red regions) and mixing coefficients are positive, this means the component was showing increased GM volume in patients. Conversely, if GM IC11 z values are negative (blue regions) and mixing coefficients are positive, this means the component was showing decreased GM volume in patients. The opposite is true when mixing coefficients are negative. A list of the regions identified in the modality-unique GM IC11 is shown in Supporting Information, Table I. Multislice views of GM IC11 can be found in Supporting Information, Figure 7B.

3.4 | Symptom correlations

In exploratory *post hoc* analyses, BPRS positive scores ($R^2 = 0.386$, $p = .010$) were significantly negatively correlated to the joint CSF IC1 mixing coefficients (Figure 5a). As shown in Figure 5b,c, GM IC7 mixing coefficients significantly positively correlated with BPRS negative scores ($R^2 = 0.281$, $p = .029$) and SANS total composite scores ($R^2 = 0.542$, $p = .003$).

Correlations between groups when comparing GM IC7 mixing coefficients with RBANS language scores ($z = 2.13$, $p = .033$; Figure 6a), RBANS attention scores ($z = 2.44$, $p = .015$; Figure 6b), and RBANS total scores ($z = 2.18$, $p = .029$; Figure 6c) were significant. It is

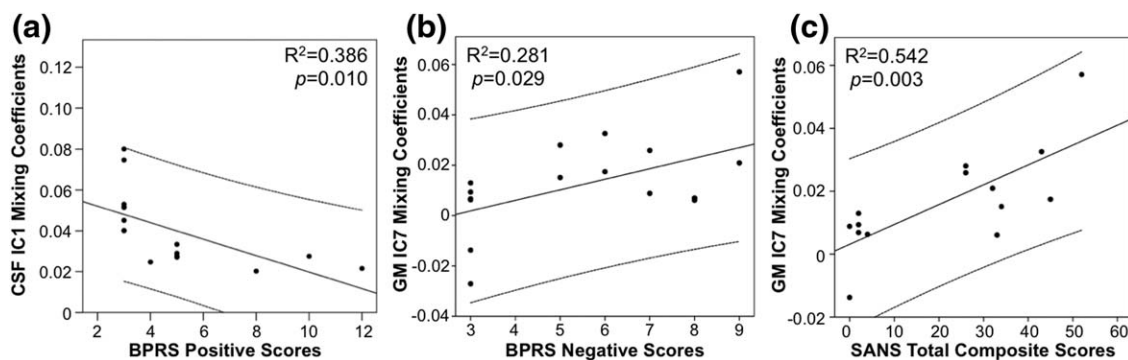


FIGURE 5 Mixing coefficient and symptom correlations. Significant correlations between (a) joint CSF IC1 mixing coefficients and BPRS positive scores, (b) GM IC7 mixing coefficients and BPRS negative scores, and (c) GM IC7 mixing coefficients and SANS total composite scores in first-episode patients with schizophrenia. CSF, cerebrospinal fluid; GM, grey matter; BPRS, Brief Psychiatric Rating Scale; SANS, Scale for the Assessment of Negative Symptoms

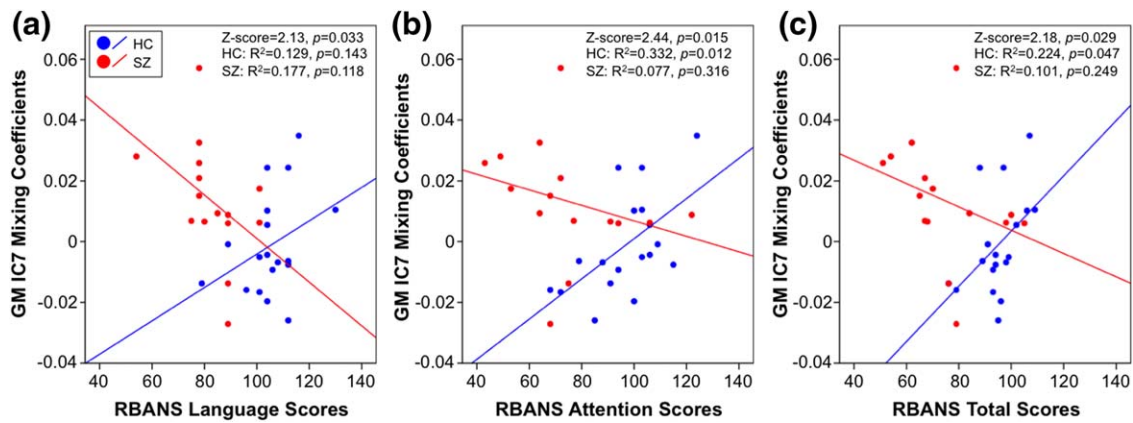


FIGURE 6 Mixing coefficient and cognitive function correlations. Correlations of GM IC7 mixing coefficients with (a) RBANS language score, (b) RBANS attention score, and (c) RBANS total score are shown. HC are represented by blue dots and SZ are represented by red dots. GM, grey matter; RBANS, Repeatable Battery for the Assessment of Neuropsychological Status; HC, healthy control; SZ, schizophrenia [Color figure can be viewed at wileyonlinelibrary.com]

important to note that within-group correlations for controls were significant when comparing GM IC7 mixing coefficients with RBANS attention scores ($R^2 = 0.332, p = .012$) and RBANS total scores ($R^2 = 0.224, p = .047$); however, within-group correlations for controls (GM IC7-RBANS language: $R^2 = 0.129, p = .143$) and patients (GM IC7-RBANS language: $R^2 = 0.177, p = .118$; GM IC7-RBANS attention: $R^2 = 0.077, p = .316$; GM IC7-RBANS total: $R^2 = 0.101, p = .249$) were not significant. Controls demonstrated additional significant positive correlations between WM IC5 mixing coefficients and RBANS visuospatial scores ($R^2 = 0.273, p = .026$) and between WM IC3 and RBANS attention scores ($R^2 = 0.283, p = .023$); however, correlations between controls and patients when comparing WM IC5 mixing coefficients with RBANS visuospatial scores ($z = 0.33, p = .741$) and WM IC3 mixing coefficients with RBANS attention scores ($z = 1.85, p = .064$) were not significant. No other significant relationships between mixing coefficients for the joint or modality-unique components and BPRS, SAPS, SANS, or RBANS scores were identified.

4 | DISCUSSION

To our knowledge, this is the first multimodal joint independent component analysis examining GM, WM, CSF, and ALFF in first-episode patients with schizophrenia at 7T. We describe distinct GM and WM abnormalities in patients with schizophrenia, as well as shared or joint abnormalities between GM and CSF, WM and ALFF, and GM and ALFF. The identified joint group-discriminative components suggest abnormalities in regions within the basal ganglia, somatosensory cortex, thalamus, frontal lobe, temporal lobe, parietal lobe, occipital lobe and ventricles, which are all regions implicated in the disorder of schizophrenia (Hadley et al., 2014; Hutcherson, Clark, Bolding, White, & Lahti, 2014; Kraguljac et al., 2016).

The joint component abnormalities indicate potential underlying associations in schizophrenia (i.e., abnormalities in one modality are potentially related to and/or driving changes in another modality) (Sui

et al., 2013b). These shared associations between modalities are not obtainable via single-modality analyses and thus emphasize the importance of implementing this type of analysis to examine the complex disorder of schizophrenia.

IC1 significantly differentiated between patients and controls in GM and CSF suggesting abnormalities in the putamen, parietal lobe, insula, thalamus, and lateral ventricles. Deficits in the putamen are supported by previous studies demonstrating increases in putamen volume in schizophrenia patients (Ellison-Wright et al., 2008; Navari & Dazzan, 2009; Shihabuddin et al., 1998). These alterations in basal ganglia volume are thought to be attributable to antipsychotic medication effects (Navari & Dazzan, 2009). Abnormalities in the parietal lobe were found within the postcentral gyrus or the location of the primary somatosensory cortex. These postcentral gyrus abnormalities are consistent with previous studies in schizophrenia patients (Glahn et al., 2008; Job et al., 2002; Zhou et al., 2007). Additionally, the abnormalities in GM volume found in the postcentral gyrus, insula, thalamus, and putamen are corroborated by results from previously published meta-analyses of GM anomalies in schizophrenia (Ellison-Wright et al., 2008; Glahn et al., 2008; Hajjma et al., 2013). Furthermore, the identified abnormalities in the somatosensory cortex, putamen, and thalamus supports the notion of thalamocortico-striatal circuit dysfunction in schizophrenia (Ellison-Wright et al., 2008). Parietal lobe abnormalities were also illustrated in the precuneus and angular gyrus in GM IC1. These findings are supported by reports of parietal lobe deficits in schizophrenia (Zhou et al., 2007). Another notable abnormality found within GM IC1 lies within the insula. These abnormalities may reflect GM insular volume or concentration loss often found to be characteristic of patients with schizophrenia (Bora et al., 2011; Chan, Di, McAlonan, & Gong, 2011; Hulshoff Pol et al., 2001; Shepherd, Laurens, Matheson, Carr, & Green, 2012; Sigmundsson et al., 2001; Wylie & Tregellas, 2010). GM IC1 abnormalities are also exhibited in the occipital gyrus, which may be indicative of characteristic deficits in visual processing in schizophrenia (Butler, Silverstein, & Dakin, 2008; Reavis et al., 2017; Schultz et al., 2013). Lateral ventricle abnormalities predominantly characterize

abnormalities exhibited in CSF IC1. These results are supported by previous first-episode schizophrenia studies demonstrating increases in ventricular volume (DeLisi, 2008; Steen, Mull, McClure, Hamer, & Lieberman, 2006; Vita, De Peri, Silenzi, & Dieci, 2006).

The regions identified with distinguished structural clarity in GM IC1 define a subcortical–cortical set of regions sharing variances with CSF abnormalities. Furthermore, the joint nature of IC1 suggests that these GM regions are influenced by lateral ventricle CSF volumes, and that these regions may be altered in schizophrenia. Indeed, these findings are supported by a previous study that has demonstrated a relationship between enlarged ventricular size and GM volume alterations across the brain (Horga et al., 2011).

Moreover, WM and ALFF IC5 is another identified joint component, which demonstrates abnormalities in the cerebellum, temporal gyrus, and visual regions including the calcarine sulcus. The temporal gyrus abnormalities found in ALFF IC5 demonstrate the importance of the temporal gyrus in the pathophysiology of schizophrenia (Ragland, Yoon, Minzenberg, & Carter, 2007). More specifically, the abnormalities in the middle temporal gyrus may be indicative of the cognitive deficits reported in schizophrenia (Ragland et al., 2007). Occipital lobe abnormalities, including part of the optic radiation, in WM IC5 may indicate dysfunction in the visual processing pathways, which is manifested through various visual perception deficits found in schizophrenia (Butler et al., 2008; Reavis et al., 2017; Schultz et al., 2013). In addition to temporal lobe abnormalities, WM IC5 also illustrated frontal lobe (middle frontal gyrus) abnormalities. Together, these abnormalities are in agreement with the frontotemporal WM abnormalities described in schizophrenia (Whitford et al., 2007; Witthaus et al., 2008). WM IC5 cerebellum abnormalities add further support to the hypothesis that the cerebellum is structurally and functionally abnormal in schizophrenia (Andreasen & Pierson, 2008). It is important to note that the field of view in our functional data did not include the cerebellum. Therefore, future functional studies examining this region at 7 T would further aid in determining potential functional abnormalities. The joint nature of IC5 in WM and ALFF suggests that function in ALFF temporal lobe regions may be influenced by WM structure within the occipital lobe and cerebellum, and that these regions may be altered in schizophrenia.

IC7 in GM and ALFF was also identified as a joint component and suggests abnormalities in the caudate, calcarine sulcus, lingual gyrus, temporal lobe, and frontal lobe regions. GM abnormalities found within the frontal and temporal lobes are reported throughout the literature [see (Birur, Kraguljac, Shelton, & Lahti, 2017; Shepherd et al., 2012) for review] and support our GM IC7 findings in the middle frontal gyrus, inferior temporal gyrus, and fusiform gyrus. These GM frontal and temporal lobe abnormalities lend support to the frontotemporal dysconnectivity hypothesis of schizophrenia proposed throughout the literature (Friston & Frith, 1995; Pettersson-Yeo, Allen, Benetti, McGuire, & Mechelli, 2011; Whitford et al., 2007). GM alterations in the occipital lobe, more specifically the calcarine sulcus and lingual gyrus, are exhibited in IC7. Again, this may be evidence of the deficits in visual processing reported in the schizophrenia literature (Butler et al., 2008; Reavis et al., 2017; Schultz et al., 2013). Similar to GM IC1,

GM IC7 also demonstrated parietal lobe abnormalities (i.e., precuneus, inferior parietal lobule, angular gyrus) consistent with the literature (Zhou et al., 2007).

Lui et al. (2010) examined the effects of antipsychotic treatment in drug-naïve first-episode patients with schizophrenia. After 6 weeks of risperidone monotherapy, patients exhibited increased ALFF in comparison to controls in the caudate (Hadley et al., 2014; Lui et al., 2010), which supports our results (ALFF IC7) examining first-episode patients treated with antipsychotic medications. These findings substantiate the importance of the caudate in schizophrenia and its role in treatment response (Hutcheson et al., 2014). Moreover, GM IC7 frontal, temporal, and occipital lobe regions may share an underlying relationship with caudate function in ALFF IC7, and may be abnormal in schizophrenia.

WM and GM abnormalities were additionally characterized via the identified modality-unique group-differentiating components. WM IC3 demonstrated abnormalities within the brainstem, internal capsule, frontal lobe, and temporal lobe. In comparison, GM IC11 exhibited abnormalities within the temporal and frontal lobes. WM IC3 brainstem abnormalities could be indicative of the role the dopaminergic neurons in the brainstem play in thalamocortico-striatal circuit dysfunction implicated in schizophrenia (Ellison-Wright et al., 2008). Furthermore, internal capsule abnormalities demonstrated in WM IC3 are supported by the literature (Di, Chan, & Gong, 2009; Horga et al., 2011; Lyu et al., 2015; Reid, White, Kraguljac, & Lahti, 2016). In fact, Horga and colleagues proposed that alterations in internal capsule could be a result of ventricular expansion consistently demonstrated in schizophrenia (Horga et al., 2011). Additionally, frontal and temporal lobe abnormalities are exhibited in both WM IC3 and GM IC11. These regions have previously been found to be abnormal in schizophrenia (Colombo et al., 2012; Di et al., 2009; Ellison-Wright et al., 2008; Fornito et al., 2009; Glahn et al., 2008; Kim & Jeong, 2015; Lyu et al., 2015; Onitsuka et al., 2004; Whitford et al., 2007). Frontal and temporal lobe abnormalities found in both modality-unique components lend further support to the frontotemporal dysconnectivity hypothesis of schizophrenia (Friston & Frith, 1995; Pettersson-Yeo et al., 2011; Whitford et al., 2007).

The significant between-group correlation of the joint GM IC7 mixing coefficients and RBANS language and attention scores may be representative of the role the frontal lobe has in the cognitive function deficits often implicated in schizophrenia (see Ragland et al., 2007 for review). GM IC7 was also characterized by inferior parietal and lingual gyrus abnormalities. A study by Weinberg and colleagues support these results as they consistently found inferior parietal deficits across three different cognitive subtypes of schizophrenia; however, they also showed lingual gyrus abnormalities between the three cognitive subtypes therefore providing further evidence for the impact heterogeneity has in characterizing the disorder (Weinberg et al., 2016). In addition, the positive correlation between GM IC7 mixing coefficients and negative symptom scores (i.e., BPRS negative scores and SANS total composite scores; Figure 5b,c) may indicate dorsal striatal dysfunction often exhibited in schizophrenia and its role in the manifestation of negative symptoms (Barch & Dowd, 2010; Ehrlich et al., 2012; Mucci et al., 2015). It is remarkable that both negative and cognitive symptoms are related to the GM IC7. Hence, poorer cognitive

symptoms and more severe negative symptoms are associated with a decrease in GM volume in the visual cortex and an increase in ALFF in the caudate. The significant relationship between CSF IC1 mixing coefficients and BPRS positive symptom scores is supported by the literature demonstrating a relationship between ventricular size and symptom type (Andreasen, Olsen, Dennert, & Smith, 1982).

Several strengths and limitations should be considered in the interpretation of our results. To minimize the variance in the data, subjects were matched based on factors such as age, gender, parental SES and smoking status. Utilization of a mCCA + jICA model requires feature extraction from each examined imaging modality. Therefore, there is a loss of information when using these features of modalities rather than the raw preprocessed data; however, the extracted features are also more manageable and interpretable than working with the high-dimensional data (Calhoun & Adali, 2009; Sui et al., 2013b). Additionally, utilization of a mCCA + jICA model indicates associations between multiple modalities via joint components. Therefore, abnormalities found in one modality may impact abnormalities in another modality. These shared, as well as unique, associations are not otherwise obtainable with single-modality analyses. One limitation to our study is the lack of multiple comparison corrections when determining significant components using multiple independent samples *t* tests. Due to the data-driven exploratory nature rather than hypothesis-driven nature of our analyses, multiple independent samples tests were not corrected for multiple comparisons. In addition, we believe the replication of our data throughout the schizophrenia literature and the distinguished structural clarity of our components (see Supporting Information, tables) are further indication of the identified components' importance. ALFF abnormalities may be dependent upon frequency range examined (Yu et al., 2014), and therefore results may be impacted as a frequency range of 0.01–0.08 Hz was utilized to calculate ALFF in this study. A sample of medicated first-episode patients with schizophrenia was examined, and therefore medication effects on brain morphology and function cannot be distinguished from intrinsic disorder characteristics. Controlling for medication types in future analyses would enable examination of the effects of medication on component results. While examination of WM volume indicates numerous alterations in WM in patients with schizophrenia, utilization of DTI (i.e., fractional anisotropy, mean diffusivity, axial/radial diffusivity) may give a more comprehensive representation of WM tract abnormalities and their relationship to GM, CSF, and ALFF. Findings may be impacted by the segmentation preprocessing pipeline used and ultimately the examination of GM/WM/CSF volume instead of concentration (Fornito et al., 2009). Although modulation of the segmented data compensates for potential deformations that can occur during the spatial normalization process, Fornito and colleagues found that GM concentration differences were often much larger and more extensive than GM volume differences when examining GM differences in schizophrenia (Fornito et al., 2009). Meda et al. found similar GM volume and GM concentration difference patterns, but GM volume differences were less significant than GM concentration differences (Meda et al., 2008). These more robust GM concentration patterns were driven by variance differences (Meda et al., 2008). Therefore, future analyses examining both volume and

concentration differences would be beneficial in determining true GM/WM/CSF differences. Finally, although bias was corrected in the MPRAGE structural images, future studies utilizing 7 T would benefit from collecting MP2RAGE structural images as these images provide more homogeneous images at 7 T.

Our results replicated findings throughout the schizophrenia literature and provide potential insight into the relationships between brain function and structure. These findings are highlighted by GM basal ganglia, somatosensory, parietal lobe, and thalamus abnormalities associated with ventricular CSF volume; WM occipital and frontal lobe abnormalities associated with temporal lobe function; and GM frontal, temporal, parietal, and occipital lobe abnormalities associated with caudate function. Ultimately, this study indicates the benefits of examining multiple modalities at 7 T with joint analyses in comparison to single-modality analyses.

ACKNOWLEDGMENT

The authors thank Dr Jennifer Robinson (Auburn University) and Dr Nouha Salibi (Siemens Healthineers) for providing the submillimeter fMRI sequence.

CONFLICT OF INTEREST

Dr Adrienne Lahti, Dr Vince Calhoun, Dr Fabio Catao, Dr Nina Kraguljac, Kristin Lottman, Dr Meredith Reid, and David White declare no potential conflicts of interest.

ORCID

Kristin K. Lottman  <http://orcid.org/0000-0002-2641-5832>

Vince D. Calhoun  <http://orcid.org/0000-0001-9058-0747>

Meredith A. Reid  <http://orcid.org/0000-0003-1946-0544>

REFERENCES

- Andreasen, N. C. (1984a). *Scale for the assessment of negative symptoms (SANS)*. Department of Psychiatry, College of Medicine, The University of Iowa.
- Andreasen, N. C. (1984b). *Scale for the assessment of positive symptoms (SAPS)*. University of Iowa, Iowa City.
- Andreasen, N. C., Olsen, S. A., Dennert, J. W., & Smith, M. R. (1982). Ventricular enlargement in schizophrenia: Relationship to positive and negative symptoms. *American Journal of Psychiatry*, *139*, 297–302.
- Andreasen, N. C., & Pierson, R. (2008). The role of the cerebellum in schizophrenia. *Biological Psychiatry*, *64*, 81–88.
- Ashburner, J. (2007). A fast diffeomorphic image registration algorithm. *NeuroImage*, *38*, 95–113.
- Ashburner, J., & Friston, K. J. (2005). Unified segmentation. *NeuroImage*, *26*, 839–851.
- Barch, D. M., & Dowd, E. C. (2010). Goal representations and motivational drive in schizophrenia: The role of prefrontal–striatal interactions. *Schizophrenia Bulletin*, *36*, 919–934.
- Behzadi, Y., Restom, K., Liu, J., & Liu, T. T. (2007). A component based noise correction method (CompCor) for BOLD and perfusion based fMRI. *NeuroImage*, *37*, 90–101.

- Bell, A. J., & Sejnowski, T. J. (1995). An information-maximization approach to blind separation and blind deconvolution. *Neural Computation*, 7, 1129–1159.
- Birur, B., Kraguljac, N. V., Shelton, R. C., & Lahti, A. C. (2017). Brain structure, function, and neurochemistry in schizophrenia and bipolar disorder—a systematic review of the magnetic resonance neuroimaging literature. *NPJ Schizophrenia*, 3, 15.
- Bora, E., Fornito, A., Radua, J., Walterfang, M., Seal, M., Wood, S. J., ... Pantelis, C. (2011). Neuroanatomical abnormalities in schizophrenia: A multimodal voxelwise meta-analysis and meta-regression analysis. *Schizophrenia Research*, 127, 46–57.
- Butler, P. D., Silverstein, S. M., & Dakin, S. C. (2008). Visual perception and its impairment in schizophrenia. *Biological Psychiatry*, 64, 40–47.
- Calhoun, V., Adali, T., & Liu, J. (2006a). A feature-based approach to combine functional MRI, structural MRI and EEG brain imaging data. *Conference Proceedings: Annual International Conference of the IEEE Engineering in Medicine and Biology Society. IEEE Engineering in Medicine and Biology Society. Annual Conference*, 1, 3672–3675.
- Calhoun, V. D., & Adali, T. (2009). Feature-based fusion of medical imaging data. *IEEE Transactions on Information Technology in Biomedicine: A Publication of the IEEE Engineering in Medicine and Biology Society*, 13, 711–720.
- Calhoun, V. D., Adali, T., Giuliani, N. R., Pekar, J. J., Kiehl, K. A., & Pearson, G. D. (2006b). Method for multimodal analysis of independent source differences in schizophrenia: Combining gray matter structural and auditory oddball functional data. *Human Brain Mapping*, 27, 47–62.
- Calhoun, V. D., & Sui, J. (2016). Multimodal fusion of brain imaging data: A key to finding the missing link(s) in complex mental illness. *Biological Psychiatry: Cognitive Neuroscience and Neuroimaging*, 1, 230–244.
- Carpenter, W. T., Jr., Gold, J. M., Lahti, A. C., Queern, C. A., Conley, R. R., Bartko, J. J., ... Appelbaum, P. S. (2000). Decisional capacity for informed consent in schizophrenia research. *Archives of General Psychiatry*, 57, 533–538.
- Chan, R. C., Di, X., McAlonan, G. M., & Gong, Q. Y. (2011). Brain anatomical abnormalities in high-risk individuals, first-episode, and chronic schizophrenia: An activation likelihood estimation meta-analysis of illness progression. *Schizophr Bulletin*, 37, 177–188.
- Colombo, R. R., Schaufelberger, M. S., Santos, L. C., Duran, F. L., Menezes, P. R., Sczufca, M., ... Zanetti, M. V. (2012). Voxelwise evaluation of white matter volumes in first-episode psychosis. *Psychiatry Research*, 202, 198–205.
- Correa, N. M., Li, Y. O., Adali, T., & Calhoun, V. D. (2008). Canonical correlation analysis for feature-based fusion of biomedical imaging modalities and its application to detection of associative networks in schizophrenia. *IEEE Journal of Selected Topics in Signal Processing*, 2, 998–1007.
- DeLisi, L. E. (2008). The concept of progressive brain change in schizophrenia: Implications for understanding schizophrenia. *Schizophrenia Bulletin*, 34, 312–321.
- Di, X., Chan, R. C., & Gong, Q. Y. (2009). White matter reduction in patients with schizophrenia as revealed by voxel-based morphometry: An activation likelihood estimation meta-analysis. *Progress in Neuro-Psychopharmacology & Biological Psychiatry*, 33, 1390–1394.
- Ehrlich, S., Yendiki, A., Greve, D. N., Manoach, D. S., Ho, B. C., White, T., ... Holt, D. J. (2012). Striatal function in relation to negative symptoms in schizophrenia. *Psychological Medicine*, 42, 267–282.
- Ellison-Wright, I., Glahn, D. C., Laird, A. R., Thelen, S. M., & Bullmore, E. (2008). The anatomy of first-episode and chronic schizophrenia: An anatomical likelihood estimation meta-analysis. *American Journal of Psychiatry*, 165, 1015–1023.
- Fornito, A., Yucel, M., Patti, J., Wood, S. J., & Pantelis, C. (2009). Mapping grey matter reductions in schizophrenia: An anatomical likelihood estimation analysis of voxel-based morphometry studies. *Schizophrenia Research*, 108, 104–113.
- Friston, K. J., & Frith, C. D. (1995). Schizophrenia: A disconnection syndrome? *Clinical Neuroscience (New York, N.Y.)*, 3, 89–97.
- Ganzetti, M., Wenderoth, N., & Mantini, D. (2016a). Intensity inhomogeneity correction of structural MR images: A data-driven approach to define input algorithm parameters. *Frontiers in Neuroinformatics*, 10, 10.
- Ganzetti, M., Wenderoth, N., & Mantini, D. (2016b). Quantitative evaluation of intensity inhomogeneity correction methods for structural MR brain images. *Neuroinformatics*, 14, 5–21.
- Glahn, D. C., Laird, A. R., Ellison-Wright, I., Thelen, S. M., Robinson, J. L., Lancaster, J. L., ... Fox, P. T. (2008). Meta-analysis of gray matter anomalies in schizophrenia: Application of anatomic likelihood estimation and network analysis. *Biological Psychiatry*, 64, 774–781.
- Hadley, J. A., Nenert, R., Kraguljac, N. V., Bolding, M. S., White, D. M., Skidmore, F. M., ... Lahti, A. C. (2014). Ventral tegmental area/mid-brain functional connectivity and response to antipsychotic medication in schizophrenia. *Neuropsychopharmacology*, 39, 1020–1030.
- Hajima, S. V., Van Haren, N., Cahn, W., Koolschijn, P. C., Hulshoff Pol, H. E., & Kahn, R. S. (2013). Brain volumes in schizophrenia: A meta-analysis in over 18 000 subjects. *Schizophrenia Bulletin*, 39, 1129–1138.
- Heckers, S. (2000). Neural models of schizophrenia. *Dialogues in Clinical Neuroscience*, 2, 267–279.
- Himberg, J., Hyvarinen, A., & Esposito, F. (2004). Validating the independent components of neuroimaging time series via clustering and visualization. *NeuroImage*, 22, 1214–1222.
- Horga, G., Bernacer, J., Dusi, N., Entis, J., Chu, K., Hazlett, E. A., ... Buchsbaum, M. S. (2011). Correlations between ventricular enlargement and gray and white matter volumes of cortex, thalamus, striatum, and internal capsule in schizophrenia. *European Archives of Psychiatry and Clinical Neuroscience*, 261, 467–476.
- Hulshoff Pol, H. E., Schnack, H. G., Mandl, R. C., van Haren, N. E., Koning, H., Collins, D. L., ... Kahn, R. S. (2001). Focal gray matter density changes in schizophrenia. *Archives of General Psychiatry*, 58, 1118–1125.
- Hutcherson, N. L., Clark, D. G., Bolding, M. S., White, D. M., & Lahti, A. C. (2014). Basal ganglia volume in unmedicated patients with schizophrenia is associated with treatment response to antipsychotic medication. *Psychiatry Research*, 221, 6–12.
- Job, D. E., Whalley, H. C., McConnell, S., Glabus, M., Johnstone, E. C., & Lawrie, S. M. (2002). Structural gray matter differences between first-episode schizophrenics and normal controls using voxel-based morphometry. *NeuroImage*, 17, 880–889.
- Keshavan, M. S., Tandon, R., Boutros, N. N., & Nasrallah, H. A. (2008). Schizophrenia, “just the facts”: What we know in 2008 Part 3: Neurobiology. *Schizophrenia Research*, 106, 89–107.
- Kim, G. W., & Jeong, G. W. (2015). White matter volume change and its correlation with symptom severity in patients with schizophrenia: A VBM-DARTEL study. *NeuroReport*, 26, 1095–1100.
- Kraguljac, N. V., White, D. M., Hadley, N., Hadley, J. A., Ver Hoef, L., Davis, E., & Lahti, A. C. (2016). Aberrant hippocampal connectivity in unmedicated patients with schizophrenia and effects of antipsychotic medication: A longitudinal resting state functional MRI study. *Schizophrenia Bulletin*, 42, 1046–1055.
- Lerman-Sinkoff, D. B., Sui, J., Rachakonda, S., Kandala, S., Calhoun, V. D., & Barch, D. M. (2017). Multimodal neural correlates of cognitive control in the Human Connectome Project. *NeuroImage*, 163, 41–54.

- Li, Y. O., Adali, T., & Calhoun, V. D. (2007). Estimating the number of independent components for functional magnetic resonance imaging data. *Human Brain Mapping, 28*, 1251–1266.
- Lui, S., Li, T., Deng, W., Jiang, L., Wu, Q., Tang, H., . . . Gong, Q. (2010). Short-term effects of antipsychotic treatment on cerebral function in drug-naïve first-episode schizophrenia revealed by “resting state” functional magnetic resonance imaging. *Archives of General Psychiatry, 67*, 783–792.
- Lyu, H., Hu, M., Eyler, L. T., Jin, H., Wang, J., Ou, J., . . . Guo, W. (2015). Regional white matter abnormalities in drug-naïve, first-episode schizophrenia patients and their healthy unaffected siblings. *Australian & New Zealand Journal of Psychiatry, 49*, 246–254.
- Meda, S. A., Giuliani, N. R., Calhoun, V. D., Jagannathan, K., Schretlen, D. J., Pulver, A., . . . Pearlson, G. D. (2008). A large scale (N=400) investigation of gray matter differences in schizophrenia using optimized voxel-based morphometry. *Schizophrenia Research, 101*, 95–105.
- Moser, E., Stahlberg, F., Ladd, M. E., & Trattnig, S. (2012). 7-T MR—from research to clinical applications? *NMR in Biomedicine, 25*, 695–716.
- Mucci, A., Dima, D., Soricelli, A., Volpe, U., Bucci, P., Frangou, S., . . . Maj, M. (2015). Is avolition in schizophrenia associated with a deficit of dorsal caudate activity? A functional magnetic resonance imaging study during reward anticipation and feedback. *Psychological Medicine, 45*, 1765–1778.
- Navari, S., & Dazzan, P. (2009). Do antipsychotic drugs affect brain structure? A systematic and critical review of MRI findings. *Psychological Medicine, 39*, 1763–1777.
- Nurnberger, J. I., Jr., Blehar, M. C., Kaufmann, C. A., York-Cooler, C., Simpson, S. G., Harkavy-Friedman, J., . . . Reich, T. (1994). Diagnostic interview for genetic studies. Rationale, unique features, and training. *NIMH Genetics Initiative. Archives of General Psychiatry, 51*, 849–859. discussion 863–4.
- Onitsuka, T., Shenton, M. E., Salisbury, D. F., Dickey, C. C., Kasai, K., Toner, S. K., . . . McCarley, R. W. (2004). Middle and inferior temporal gyrus gray matter volume abnormalities in chronic schizophrenia: An MRI study. *American Journal of Psychiatry, 161*, 1603–1611.
- Overall, J. E., & Gorham, D. R. (1962). The brief psychiatric rating scale. *Psychological Reports, 10*, 799–812.
- Pettersson-Yeo, W., Allen, P., Benetti, S., McGuire, P., & Mechelli, A. (2011). Dysconnectivity in schizophrenia: Where are we now? *Neuroscience and Biobehavioral Reviews, 35*, 1110–1124.
- Poser, B. A., & Norris, D. G. (2009). Investigating the benefits of multi-echo EPI for fMRI at 7 T. *NeuroImage, 45*, 1162–1172.
- Ragland, J. D., Yoon, J., Minzenberg, M. J., & Carter, C. S. (2007). Neuroimaging of cognitive disability in schizophrenia: Search for a pathophysiological mechanism. *International Review of Psychiatry, 19*, 417–427.
- Randolph, C., Tierney, M. C., Mohr, E., & Chase, T. N. (1998). The Repeatable Battery for the Assessment of Neuropsychological Status (RBANS): Preliminary clinical validity. *Journal of Clinical and Experimental Neuropsychology, 20*, 310–319.
- Reavis, E. A., Lee, J., Wynn, J. K., Narr, K. L., Njau, S. N., Engel, S. A., & Green, M. F. (2017). Linking optic radiation volume to visual perception in schizophrenia and bipolar disorder. *Schizophrenia Research*.
- Reid, M. A., White, D. M., Kraguljac, N. V., & Lahti, A. C. (2016). A combined diffusion tensor imaging and magnetic resonance spectroscopy study of patients with schizophrenia. *Schizophrenia Research, 170*, 341–350.
- Schultz, C. C., Wagner, G., Koch, K., Gaser, C., Roebel, M., Schachtzabel, C., . . . Schlosser, R. G. (2013). The visual cortex in schizophrenia: Alterations of gyrification rather than cortical thickness—a combined cortical shape analysis. *Brain Structure and Function, 218*, 51–58.
- Shepherd, A. M., Laurens, K. R., Matheson, S. L., Carr, V. J., & Green, M. J. (2012). Systematic meta-review and quality assessment of the structural brain alterations in schizophrenia. *Neuroscience and Biobehavioral Reviews, 36*, 1342–1356.
- Shihabuddin, L., Buchsbaum, M. S., Hazlett, E. A., Haznedar, M. M., Harvey, P. D., Newman, A., . . . Luu-Hsia, C. (1998). Dorsal striatal size, shape, and metabolic rate in never-medicated and previously medicated schizophrenics performing a verbal learning task. *Archives of General Psychiatry, 55*, 235–243.
- Sigmundsson, T., Suckling, J., Maier, M., Williams, S., Bullmore, E., Greenwood, K., . . . Toone, B. (2001). Structural abnormalities in frontal, temporal, and limbic regions and interconnecting white matter tracts in schizophrenic patients with prominent negative symptoms. *American Journal of Psychiatry, 158*, 234–243.
- Song, X. W., Dong, Z. Y., Long, X. Y., Li, S. F., Zuo, X. N., Zhu, C. Z., . . . Zang, Y. F. (2011). REST: A toolkit for resting-state functional magnetic resonance imaging data processing. *PLoS One, 6*, e25031.
- Steen, R. G., Mull, C., McClure, R., Hamer, R. M., & Lieberman, J. A. (2006). Brain volume in first-episode schizophrenia: Systematic review and meta-analysis of magnetic resonance imaging studies. *British Journal of Psychiatry, 188*, 510–518.
- Stephen, J. M., Coffman, B. A., Jung, R. E., Bustillo, J. R., Aine, C. J., & Calhoun, V. D. (2013). Using joint ICA to link function and structure using MEG and DTI in schizophrenia. *NeuroImage, 83*, 418–430.
- Sui, J., Adali, T., Pearlson, G., Yang, H., Sponheim, S. R., White, T., & Calhoun, V. D. (2010). A CCA+ICA based model for multi-task brain imaging data fusion and its application to schizophrenia. *NeuroImage, 51*, 123–134.
- Sui, J., He, H., Pearlson, G. D., Adali, T., Kiehl, K. A., Yu, Q., . . . Calhoun, V. D. (2013a). Three-way (N-way) fusion of brain imaging data based on mCCA+jICA and its application to discriminating schizophrenia. *NeuroImage, 66*, 119–132.
- Sui, J., He, H., Yu, Q., Chen, J., Rogers, J., Pearlson, G. D., . . . Calhoun, V. D. (2013b). Combination of resting state fMRI, DTI, and sMRI data to discriminate schizophrenia by N-way MCCA + jICA. *Frontiers in Human Neuroscience, 7*, 235.
- Sui, J., Huster, R., Yu, Q., Segall, J. M., & Calhoun, V. D. (2014). Function-structure associations of the brain: Evidence from multimodal connectivity and covariance studies. *NeuroImage, 102 Pt 1*, 11–23.
- Sui, J., Pearlson, G., Caprihan, A., Adali, T., Kiehl, K. A., Liu, J., . . . Calhoun, V. D. (2011). Discriminating schizophrenia and bipolar disorder by fusing fMRI and DTI in a multimodal CCA+ joint ICA model. *NeuroImage, 57*, 839–855.
- Sui, J., Yu, Q., He, H., Pearlson, G. D., & Calhoun, V. D. (2012). A selective review of multimodal fusion methods in schizophrenia. *Frontiers in Human Neuroscience, 6*, 27.
- Tandon, R., Keshavan, M. S., & Nasrallah, H. A. (2008). Schizophrenia, “Just the Facts”: What we know in 2008 part 1: Overview. *Schizophrenia Research, 100*, 4–19.
- Tandon, R., Nasrallah, H. A., & Keshavan, M. S. (2009). Schizophrenia, “just the facts” 4. Clinical features and conceptualization. *Schizophrenia Research, 110*, 1–23.
- Vita, A., De Peri, L., Silenzi, C., & Dieci, M. (2006). Brain morphology in first-episode schizophrenia: A meta-analysis of quantitative magnetic resonance imaging studies. *Schizophrenia Research, 82*, 75–88.
- Wang, Z., Meda, S. A., Keshavan, M. S., Tamminga, C. A., Sweeney, J. A., Clementz, B. A., . . . Pearlson, G. D. (2015). Large-scale fusion of gray matter and resting-state functional MRI reveals common and distinct biological markers across the psychosis spectrum in the B-SNIP cohort. *Frontiers in Psychiatry, 6*, 174.

- Weinberg, D., Lenroot, R., Jacomb, I., Allen, K., Bruggemann, J., Wells, R., ... Weickert, T. W. (2016). Cognitive subtypes of schizophrenia characterized by differential brain volumetric reductions and cognitive decline. *JAMA Psychiatry*, *73*, 1251–1259.
- Weiskopf, N., Lutti, A., Helms, G., Novak, M., Ashburner, J., & Hutton, C. (2011). Unified segmentation based correction of R1 brain maps for RF transmit field inhomogeneities (UNICORT). *NeuroImage*, *54*, 2116–2124.
- Whitfield-Gabrieli, S., & Nieto-Castanon, A. (2012). Conn: A functional connectivity toolbox for correlated and anticorrelated brain networks. *Brain Connectivity*, *2*, 125–141.
- Whitford, T. J., Grieve, S. M., Farrow, T. F., Gomes, L., Brennan, J., Harris, A. W., ... Williams, L. M. (2007). Volumetric white matter abnormalities in first-episode schizophrenia: A longitudinal, tensor-based morphometry study. *American Journal of Psychiatry*, *164*, 1082–1089.
- Witthaus, H., Brune, M., Kaufmann, C., Bohner, G., Ozgurdal, S., Gudlowski, Y., ... Juckel, G. (2008). White matter abnormalities in subjects at ultra high-risk for schizophrenia and first-episode schizophrenic patients. *Schizophrenia Research*, *102*, 141–149.
- Wylie, K. P., & Tregellas, J. R. (2010). The role of the insula in schizophrenia. *Schizophrenia Research*, *123*, 93–104.
- Yu, R., Chien, Y. L., Wang, H. L., Liu, C. M., Liu, C. C., Hwang, T. J., ... Tseng, W. Y. (2014). Frequency-specific alternations in the amplitude of low-frequency fluctuations in schizophrenia. *Human Brain Mapping*, *35*, 627–637.
- Zhou, S. Y., Suzuki, M., Takahashi, T., Hagino, H., Kawasaki, Y., Matsui, M., ... Kurachi, M. (2007). Parietal lobe volume deficits in schizophrenia spectrum disorders. *Schizophrenia Research*, *89*, 35–48.

SUPPORTING INFORMATION

Additional Supporting Information may be found online in the supporting information tab for this article.

How to cite this article: Lottman KK, White DM, Kraguljac NV, et al. Four-way multimodal fusion of 7 T imaging data using an mCCA+jICA model in first-episode schizophrenia. *Hum Brain Mapp*. 2018;39:1475–1488. <https://doi.org/10.1002/hbm.23906>